РАДІАЦІЙНА ФІЗИКА
RADIATION PHYSICS

УДК 533.924+538.97 https://doi.org/10.15407/jnpae2021.04.358

L. Jadoual[1], A. Afkir[1], A. El Boujlaidi[1], M. Ait El Fqih[2,*], R. Jourdani[1], A. Kaddouri[1]

[1] *Laboratory of Materials, Energy, and Environment, Cadi Ayyad University, Marrakech, Morocco*
[2] *Laboratory of Artificial Intelligence & Complex Systems Engineering, ENSAM, Hassan II University of Casablanca, Casablanca, Morocco*

*Corresponding author: m.aitelfqih@gmail.com

ION-PHOTON EMISSION FROM TITANIUM TARGET UNDER ION BEAM SPUTTERING

Ion photon emission in the wavelength range of 280 - 420 nm resulting from 5 Kr^+ ion beam sputtering from titanium in the presence and the absence of oxygen was studied experimentally. The observed spectra consist of a series of discrete lines superimposed with a broadband continuum. Discrete lines are attributed to excited neutral Ti I and excited ions Ti II. The differences in the observed intensities of spectral lines are discussed in terms of the electron-transfer processes between the excited sputtered atom and electronic levels of the solid. The radiative dissociation process and breaking of chemical bonds seem to contribute to the enhancement of emitted photons intensity. Continuum radiation was observed and is very probably related to the electronic structure of titanium. The collective deactivation of 3d-shell electrons appears to play a role in the emission of this radiation.

Keywords: sputtering, titanium, light emission, electron-transfer model, continuum radiation.

1. Introduction

During the last decades, the interaction of low-energy heavy ions with solid surfaces plays a main role in a wide range of scientific and technological problems and remains an active area for research [1, 2]. Comparative analysis of spectra from ion-atom, ion-solid, and ion-surface collisions provides the opportunity to extract detailed information about the basic collision mechanism leading to excited-state formation [3, 4]. In particular, one of such events resulting from ion beam sputtering is light emission. This kind of radiation can provide some information about the mechanism of excitation and de-excitation in front of bombarded surfaces [5, 6].

Excitation in sputtering with an oxygen atmosphere is much more complicated and even less understood in the case of targets from transition metal [7]. Explanations of the excited state populations in terms of direct excitation in atom-atom collisions in the cascade, atom-surface electron transfer, bond breaking, and the local thermal equilibrium processes have been proposed so far [8]. The intensity was enhanced by orders of magnitude when the silicium surface was covered with oxygen and interpreted within a model for the overlap of the individual collision cascades. Dogar et al. [9] assumed that the dominating effect in the production of excited atoms and ions during the bombardment of $YBaCu_3O_7$ by 1 - 10 Ar^+ ions is the electron exchange mechanism between sputtered particle and surface. Fournier et al. [10] bombarded $YBa_2Cu_3O_7$ superconductors at room temperature and 10 K by 5 keV Kr^+ ions and they observed discrete lines attributed to neutral excited cuprum, barium, and a few lines attributed to ionic barium and yttrium superimposed to a small continuum related to the oxide. Recently, Ait El Fqih et al. studied the experimental results of the light emission from sputtered atoms from clean cuprum and aluminium and from three alloys with different concentrations [11].

The present work highlights ion-photon emission of clean titanium under 5 keV Kr^+ ion bombardment. The influence of oxygen on these optical emissions was well emphasized. The difference in photon yield, from clean titanium in the absence and the presence of oxygen, is discussed in terms of the electron-transfer process. This model explains the enhancement of the photon emission caused by O_2 covered surface (oxygenated titanium). We have successfully validated this model for silicon [12] and vanadium [13] and recently for nickel [14] and chromium [15].

2. Experimental

The apparatus for light emission study has been described in earlier papers [16, 17]. Briefly, 5 keV Kr^+ ions were produced by electron impact on krypton gas (of 99.998 % purity) in a cold plasma source. The gas pressure in the target chamber was raised better than 10^{-7} torr in the absence of oxygen and 10^{-5} torr in the presence of oxygen. The gas pressure was measured by a Penning gauge (CF 2P).

The beam section was estimated to be 1.6 mm², giving a current density of about 1 μA/mm^2 at an incident angle of 65° with respect to the normal surface which maximizes the sputtering yield. The appearance of continuous radiation is connected with the registration of luminescence. The analysis of the emitted light was performed using the R320 Jobin Yvon monochromator equipped with 1800 groves/mm holographic grating using a variable slit width. The range of the spectrograph extends from 190 to 650 nm with a spectral resolution better than 0.2 nm. Hamamatsu 4220P photomultiplier was employed to explore wave-length range. A micro-computer was used with the PRISM program to control the whole detection system and to collect data.

Polycrystalline titanium with purity > 99 % was prepared by mechanical polishing and ultrasonic cleaning in ethanol and then placed in an ultra-high vacuum (better than 10^{-7} torr). The erosion velocity was then of the order of 10 nm/s has also been reported by Fournier et al. [18].

3. Results and discussion

During ion beam sputtering, three most classes of emitted radiation were found. The first dominant emission was the discrete lines due to excited atoms or atomic ions [19]. In the second, which is much less usual, the emission occurs from excited molecular species, usually Me-H (Me: metal) [20] or Me-O [21]. In the third, the broad-band radiation (so-called continuum radiation) is also found. This kind of radiation was generally attributed to the excited Me_nO_m molecules produced in the collision cascade [22]. El Boujlaidi et al. [23] have studied the continuum radiation emitted from transition metals under ion bombardment and have proposed that emission depends on the nature of the metal and is very probably related to its electronic structure.

3.1. Discrete emission

Typical spectra of ion-photon emission in the spectra range between 280 and 420 nm emitted during sputtering of polycrystalline titanium, in the absence (Fig. 1, *a*) and the presence of oxygen (Fig. 1, *b*) targets by Kr^+ ions with 5 keV are presented.

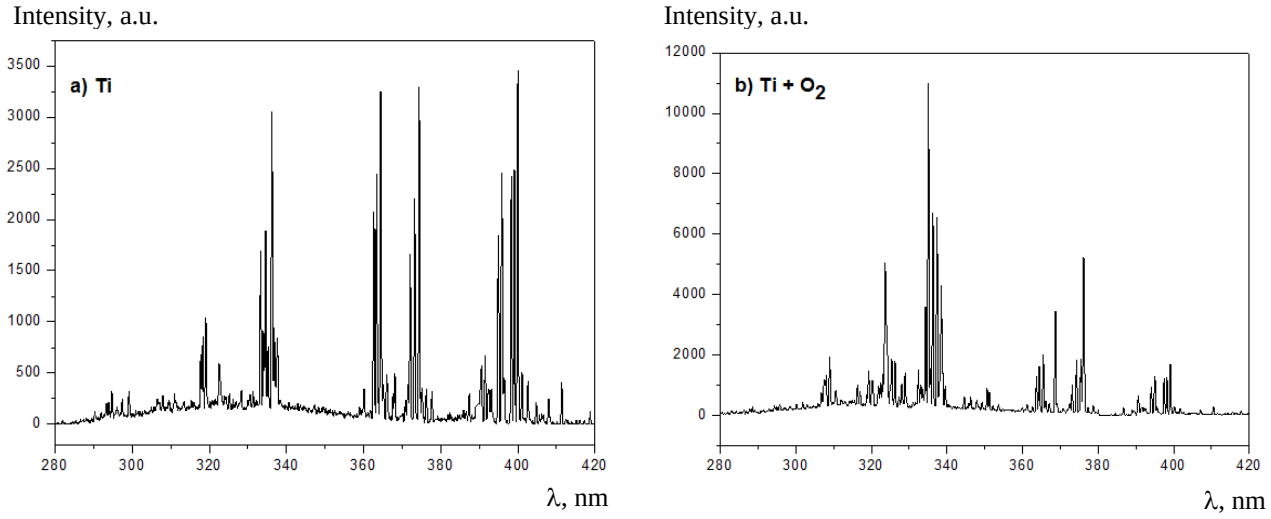

Fig. 1. Optical spectra in the range (280 - 420 nm) of:
a – clean titanium target; *b* – oxygenated titanium; bombarded by 5 keV Kr^+ ions.

The optical spectra are measured with a resolution of 0.2 nm and contain a multitude of discrete lines superimposed on a continuum. Discrete emission lines were identified by consulting the literature data [24]. These spectra present the Ti I lines attributed to neutral atoms and Ti II lines of ionic atoms. In the case of clean titanium (in the absence of oxygen), the most intense line is located at 402.62 nm from the transition $3d^24pz^4G_{7/2}$ - $3d^24sa^2F_{7/2}$. In the presence of oxygen, the most intense line is located at 335.15 nm and is attributed to Ti I line with the transition $3d^24s6sh^5F_2$ - $3d^24s4pz^5G°_3$. In clean titanium, the observed discrete lines are due to the de-excitation of particles, which have escaped to non-radiative processes. In fact, an exciting atomic particle located at the distances very close to the target is an unstable system. It can deactivate rapidly by non-radiative processes such as the Auger (de-excitation or neutralization) or resonance (neutralization or ionization) processes. Subsequently, these processes compete with de-excitation by photon emission. The survival probability of an excited atom escaping from the target without undergoing a radiationless de-excitation to be given by [25]:

$$P(s,v_\perp)=\exp\left[\frac{A}{av_\perp}\left(e^{-as}-1\right)\right]$$

and for long distances by:

$$P(s,v_\perp)=\exp\left[-\frac{A}{av_\perp}\right],$$

where $v_\perp$ is perpendicular to the surface component of the velocity vector of the ejected particle. A and a are constants characteristic of the involved process. For Auger and resonance processes, the ratio of these constants reported by Terzic and Perovic [26] was A/a = $5\cdot10^{13}$ – $5\cdot10^{15}$ Å/s. The probability is about 0.8 for particles ejected from titanium with an energy of 1 keV. Thus, for the clean titanium target, the light emission was likely due to the fast particles which deactivate away from the surface to escape to non-radiative processes.

Tables 1 and 2 depict experimental spectral results. In the first column, we mentioned the observed wavelength λ_o of Ti I and Ti II lines respectively. The literature wavelength λ_L is reported in column 2 [24]. The absolute intensity of spectral lines from clean and oxygenated titanium (Ti + O_2) was reported in columns 3 and 4, respectively. The dependence and identification of the transition responsible for the emission of energies (eV) of the upper and lower electronic states implied in this transition are given in columns 5 and 6, respectively. The value indicated for the higher state gives the internal energy of excited atoms. Columns 7, 8, and 9 present the energies of the emitted states of spectral Ti I and Ti II lines and are determined by the values of E_v, given by $E_v = E^* - I^{n+}$, where E^* is the energy of the excited states. The value of the ionization potential of the titanium atom is (Ti) = 6.83 eV and the value of the ionization potential of the single-charged titanium ion is (Ti) = 13.58 eV. In the last column of Table 1, we labeled from a to m the different Ti I lines corresponding to indicated E_v.

Table 1. **The wavelength and absolute intensity of observed emission lines and their assignment and attributed to the Ti I lines**

λ_0, nm Observed	λ_L, nm [24]	Intensity, a.u.		Dependence	Transition [24]	Energy levels, eV [24]			
		Clean Ti ($P < 10^{-7}$ torr)	Ti + O_2 ($P = 10^{-5}$ torr)			Upper, eV	Lower, eV	E_v, eV	Ti I lines
297.52	297.46 Ti I	245	230	0	$3d^24s5p^3F^\circ_4$ - $3d^34sa^3G_4$	6.04	1.88	–0.79	a
306.60	306.52Ti I	250	625	+	$3d^24s5p^3G^\circ_3$ - $3d^24s^2a^3F_2$	5.47	0.00	–1.36	b
310.91	310.74 Ti I	300	325	0	$3d^24p^2\,^5F_1$ - $3d^2\,^3F_14s4p3P^\circ z5G^\circ_2$	5.95	1.96	–0.88	c
319.40	319.29 Ti I	720	1410	+	$3d^3\,^4F_4pw^3G_4$ - $3d^24s^2a^3F_3$	3.90	0.02	–2.93	d
324.49	324.47 Ti I	270	1450	+	$3d^2\,^3P4s4p^3P^\circ v^3D^\circ_3$ - $3d^24sa^3F_4$	3.86	0.04	–2.97	e
333.26	333.15 Ti I	880	910	0	$3d^24s6sh^5F_3$ - $3d^24s4pz^5G^\circ_2$	5.69	1.97	–1.14	f
334.00	333.99 Ti I	910	1370	+	$3d^35p\,^3G^\circ_4$ - $3d^34sa^3G_4$	5.59	1.88	–1.24	g
334.60	334.43 Ti I	1855	1865	0	$3d^24s6sh^5F_4$- $3d^2\,4s4pz^5G^\circ_4$	5.70	1.99	–1.13	h
335.33	335.15 Ti I	625	10990	+	$3d^24s6sh^5F_2$ - $3d^24s4pz^5G^\circ_3$	5.58	1.98	–1.25	i
336.30	336.19 Ti I	3055	6375	+	$3d^24s4px^3G^\circ_3$ - $3d^24s^2a^3F_3$	3.70	0.02	–3.13	j
337.81	337.66 Ti I	845	2120	+	$3d^34p^3G^\circ_4$ - $3d^34sb^3F_3$	5.11	1.44	–1.72	k
374.96	374.92 Ti I	320	1180	+	$3d^34d^5G_6$ - $3d^24s4pz^5F^\circ_5$	5.44	2.13	–1.39	l
376.50	376.44 Ti I	351	5202	+	$3d^34py^5G^\circ_3$ -$3d^24s^2a^3F_2$	3.29	0.00	–3.54	m

Fig. 2 shows the energy diagram of titanium metal and TiO_2 oxide and oxygenated titanium (Ti + O_2). We have also reported the energy level of the free excited atoms and the associated transitions. The titanium metal is characterized by its work function ϕ(Ti) = 4.30 eV [27]. The TiO_2 oxide is characterized by its electronic affinity A_f (TiO_2) = = 1.59 eV [28] and its bandgap energy E_g (TiO_2) = = 2.50 eV [29].

It is well known that the emitted light strongly depends on the condition of the surface under ion bombardment and, therefore, forms the basis of surface chemical analysis, where the species present at the surface can be identified by their characteristic line emission. In some cases, the light intensity is found to be strongly sensitive to surface contamination (for example oxygen) [2].

In order to elucidate the behavior of the observed line intensities in the presence of oxygen, the electron-transfer model was made. This model has been well described in earlier works [29] and was successfully validated in our team for several metals [12 - 15]. Oxygen induces changes in the band structure since the measured yield is governed by

Table 2. **The wavelength and absolute intensity of observed emission lines and their assignment and attributed to the Ti II ionic lines, when titanium and Ti + O_2 are bombarded by 5 keV Kr^+**

λ_0, nm Observed	λ_L, nm [24]	Intensity, a.u.		Dependence	Transition [24]	Energy levels, eV [24]		
		Clean Ti ($P < 10^{-7}$ torr)	Ti + O_2 ($P = 10^{-5}$ torr)			Upper, eV	Lower, eV	E_v, eV
294.70	294.61 Ti II	310	285	–	$3d^24de^4G_{11/2}$ - $3d^24pz^4F°_{9/2}$	8.08	3.88	–5.55
298.33	298.31 Ti II	2420	1215	–	$3d^24pz^4G°_{7/2}$ - $3d^24sa^2F_{5/2}$	3.68	0.57	–9.90
317.70	317.55 Ti II	680	325	–	$3d^23F5se^4F_{9/2}$ - $3d^2\,{}^3F\ 4pz^4F°_{7/2}$	7.76	3.85	–5.82
362.60	362.58 Ti II	2070	285	–	$3d^24pz^2S_{1/2}$ - $3d^3a^2P_{1/2}$	4.64	1.22	–8.94
363.40	363.34 Ti II	2445	190	–	$3d^24d^4P_{3/2}$ - $3d^24pz^4S°_{3/2}$	8.37	4.96	–5.21
364.40	364.35 Ti II	3255	1640	–	$3d^24d^2G_{7/2}$ - $3d4s4p^4D°_{5/2}$	9.93	6.52	–3.65
370.80	377.60 Ti II	235	145	–	$3d^2\,{}^1D°4pz^2P°_{3/2}$ - $3d^3b^2D^2_{5/2}$	4.86	1.58	–8.72
372.30	372.27 Ti II	1120	335	–	$3d^24pz^2F°_{7/2}$ - $3d^24sa^2F_{5/2}$	3.90	0.57	–9.68
374.30	374.27 Ti II	3290	1820	–	$3d^24py^2D_{5/2}$ - $3d^3b^2D^2_{5/2}$	4.89	1.58	–8.69
377.71	377.54 Ti II	310	260	–	$3d^24pz^4F_{7/2}$ - $3d^24sa^2F_{5/2}$	3.85	0.57	–9.73
402.70	402.62 Ti II	3457	1697	–	$3d^24pz^4G_{7/2}$ - $3d^24sa^2F_{7/2}$	3.70	0.61	–9.88

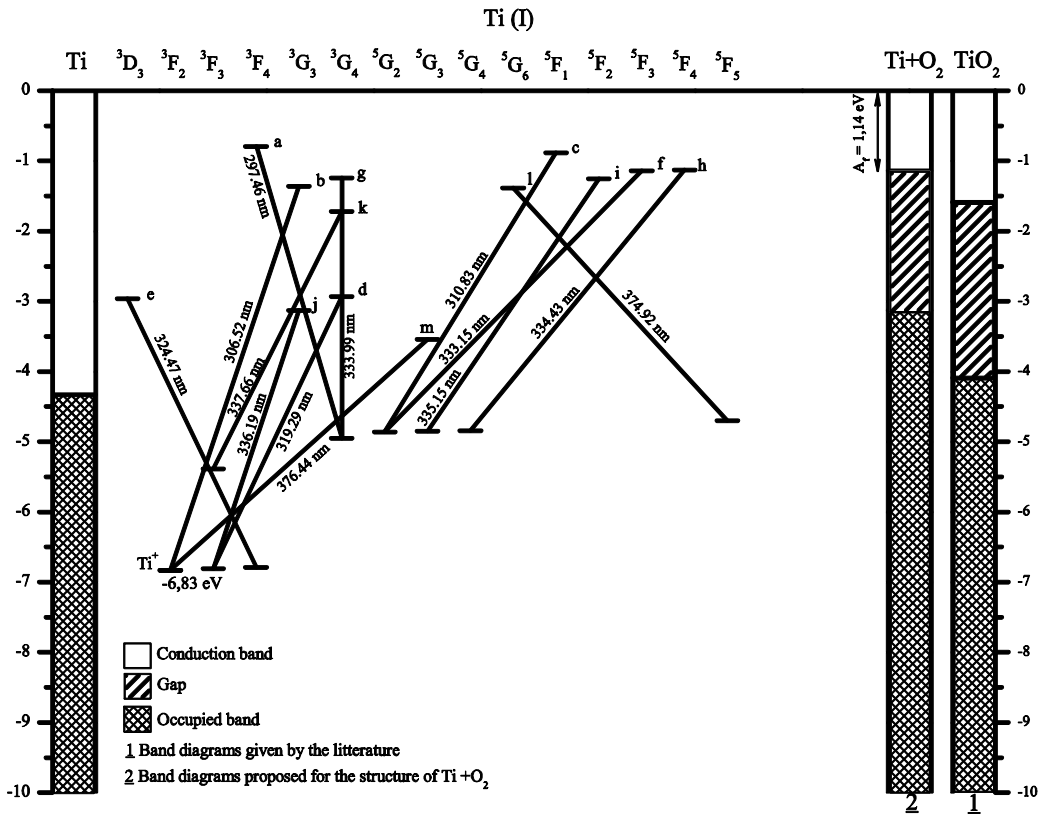

Fig. 2. Energy diagram of metal (titanium), oxide (TiO_2), and excited atoms Ti.

electron transfer processes between surface and excited sputtered atoms. The excited states of four Ti I lines (labeled a, c, f, and h) whose intensity is invariant, are located at the same time inside the energy range of the metal conduction band ($0 < |E_v| < \phi(\mathrm{Ti})$) and the oxide conduction band ($|E_v| < A_f$). These states can exchange excited electrons to the metal (titanium) and they can be also exchanged with the formed oxide. In the presence of oxygen, the deactivation of the excited states is carried out by the emission of photons, and the light signal is then enhanced; it is what we have observed for the noted states b, d, e, g, i, j, k, l, and m. In fact, electron tunneling is blocked by the bandgap, which consequently enhances the light signal. This model suggests that the formed oxide has an electronic affinity of about 1.14 eV and the gap lower than

2.40 eV corresponding to the difference of energy between two levels of energy noted m ($|E_v|$ = = 3.54 eV) and f ($|E_v|$ = 1.14 eV). The value of the bandgap is in good agreement with the measured value ($1.23 < E_g < 2.5$ eV) by Mowbray et al. [30]. In Fig. 2, the results show clearly that the structure band of the film oxide, which formed in an oxygen atmosphere, is close to that of TiO_2 but with a lower electronic affinity.

The ionic spectral Ti II lines (Ti^+) show a negative dependence on oxygen. This observation cannot be explained by the electron transfer model. Indeed, the model predicts a diminution of the intensities of the spectral lines because the correspondent ionized states can be occupied by the metal and not by the corresponding oxide. The emitting states must be located in front of the gap but also in front of the state's occupied conduction band. Afanasieva et al. [31] suggest that exciting ions arise during multiple collisions between the incoming ion and target surface atoms. This is evidenced by the high energy of the ions that fly away from the surface of the target.

This mechanism is effective by electron capture from the metal by Ti^{++} ion situated in the vicinity of the surface according to the reaction:

$$Ti^{++} + e_s^- \rightarrow Ti^{+*},$$

where e_s^- is the transferred electron from the surface. It seems that this reaction is much more favorable for the metal than the oxygenated metal. The electron capture is energetically favorable for the exciting levels that lie within the energy range of the valence band.

Nevertheless, the produced ions can be explained by the chemical model. This model is used for secondary emission of ions from oxides or metal bombarded by oxygen or by O^{2+} ions. Under this chemical model, the particle is ejected from a position where it exists naturally in the ion in the ground state, and in the output, no electron comes to neutralize [32].

3.2. Continuous radiation

During ion beam sputtering of clean and oxygenated titanium, continuous luminescence was observed in a broad wavelength range between 275 and 400 nm. The maximum was located at 325 nm (see Figs. 1 and 3). Several studies tried to understand the phenomenon of continuous radiation. Suchanska [2] attributes the broad bands to excited metal-oxide-free molecules. Oxygen and metal atoms are produced from the collision cascade because incident ions remove electrons from the

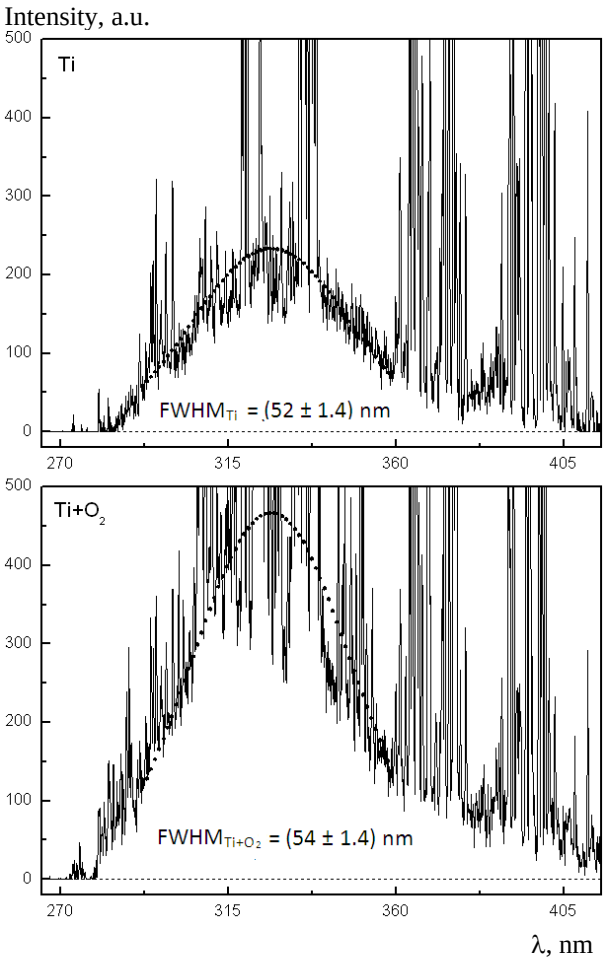

Fig. 3. Part of continuum spectra observed during 5 keV Kr^+ ion bombardment of dynamically clean titanium and titanium in the presence of oxygen.

doubly electronegative oxygen atoms. This mechanism is known in the literature as the band-breaking model and can be qualitatively described by the two-level-crossing Landau - Zener model [33]. Rausch et al. [34] argue that the continuum emission cannot be due to luminescence of the solid because the region of emission extends several millimeters in front of the surface and the emission must therefore originate from ejected particles. Fournier et al. [21] have observed a continuum emission when bombarding BeO surface with Kr^+ ions. They affect the origin of continuum radiation in two ways. Firstly, the aforementioned excitons are bulk excitons and their destiny in a thin and perturbed surface layer is problematic. Secondly, in a collision cascade, the displacements of beryllium and oxygen atoms are different, which statistically creates Frenkel defects [21]. In [35] a non-slip incident beam is considered. In the experiment, the target is located in such a way that only the radiation of flying particles reaches the entrance slit of the recording device. Qayyum et al. [36] observed a continuum structure during the sputtering of graphite targets with 1 - 10 keV Ne^+, Kr^+, and Xe^+ beams. They suggest that the observed

continuum emission during sputtering of graphite with 1 - 10 keV inert gas ions is predominantly due to the overlapping of various band systems of sputtered C_2 with small contributions from bands of heavier sputtered carbon clusters. Mass analysis showed that the intensity of C_2 was an order of magnitude higher than C_3 and C_4 in the graphite's sputtered flux. However, the increase of carbon cluster sputtering with ion beam fluence cannot be explained on the basis of these results. The continuum radiation is observed in the case of clean vanadium [23]. It is found to be enhanced by the presence of oxygen, probably due to chemisorptions. This enhancement can reach a factor of 2. In our experiments, we have observed continuous radiation. In fact, this radiation was observed for a transition metal, which the 3d shell has half occupied. Moreover, we simulated a broad-band continuum to a discrete line (Fig. 3). The full width at half maximum (FWHM) is almost identical for titanium and the oxide formed by introducing the oxygen (52 and 54 nm for clean and oxygenated titanium, respectively). Let us say that the lifetime of the continuum radiation is similarly identical in the case of titanium and Ti + O_2 structure. As a result, the origin of the continuum radiation is probably the same for titanium and the structure formed in the presence of oxygen (Ti + O_2).

4. Conclusion

In summary, photon emission is studied in the spectral range 280 - 420 nm during the bombardment of clean and oxygenated titanium by 5 keV Kr^+. The presence of oxygen affects considerably the intensity of spectral lines. We recorded that the presence of oxygen leads to the formation of an oxidized layer, which is responsible for the increase of Ti I lines of photon emission. The electron transfer model explains our experimental result concerning the observed behavior of Ti I lines. The larger band-gap of oxide favors radiative transitions leading to an enhancement of the photon yield. The radiative dissociation of sputtered titanium-oxygen molecules may also contribute to the increase of light emission of neutral atoms Ti I. Continuum radiation was also observed and this radiation depends on the nature of metal and is very probably related to its electronic structure. The collective deactivation of 3d-shell electrons appears to play a role in the emission of this radiation. The observed enhancement in the presence of oxygen is probably due to a significant contribution of the oxide molecules. Other experiments must be conducted to further elucidate the origin of this radiation.

REFERENCES

1. R. Kelly. Towards a unified model for the formation of sputtered excited states. In: *Inelastic Particle Surface Collisions*. Eds. E. Taglauer, W. Heiland (Berlin: Springer-Verlag, 1981) p. 84.
2. M. Suchanska. Ion-induced photon emission of metals. Prog. Surf. Sci. 54(2) (1997) 165.
3. J.M. Hollas. *Modern Spectroscopy*. (Chichester: Wiley, 2004).
4. H. Gnaser. Energy and Angular Distributions of Sputtered Species. In: *Sputtering by Particle Bombardment*. Eds. R. Behrisch, W. Eckstein. Topics Appl. Phys. 110 (2007) 231.
5. V.V. Bobkov et al. Mechanisms of formation of sputtered particles in excited states at Ar^+ ion bombardment of oxide targets. Nucl. Instrum. Methods B 256(1) (2007) 501.
6. N.A. Azarenkov et al. Ion-photon emission under ion bombardment of garnet structures of different composition. Vacuum 105 (2014) 91.
7. P. Agarwal, S. R. Bhattacharyya, D. Ghose. Transient effect in light emission during oxygen ion bombardment of a beryllium-copper target. Appl. Surf. Sci. 133(3) (1998) 166.
8. M.L. Yu. Charged and excited states of sputtered atoms. In: *Sputtering by Particle Bombardment*. III. Eds. R. Behrisch, K. Wittmaack. Topics Appl. Phys. 64 (1991) 91.
9. A.H. Dogar, A. Qayyum. Atomic excitations during ion beam sputtering of $YBa_2Cu_3O_7$ targets. Nucl. Instrum. Methods B 247(2) (2006) 290.
10. J. Fournier et al. Optical spectroscopy analysis of $YBa_2Cu_3O_7$ at room temperature and at 10 K. J. Appl. Phys. 69 (1991) 2382.
11. M. Ait El Fqih et al. Bombardment-induced light emission of clean and oxygen-covered Al, Cu, and Cu_x Al_{1-x} targets. Surf. Interface Anal. 50(10) (2018) 969.
12. A. Kaddouri et al. Photon emission from clean and oxygenated Si and SiO_2 surfaces bombarded by 5 keV krypton ions. Appl. Surf. Sci. 256 (2009) 116.
13. M. Ait El Fqih et al. On the validity of the electron transfer model in photon emission from ion bombarded vanadium surfaces. Eur. Phys. J. D 63 (2011) 97.
14. L. Jadoual et al. Optical Emission from Ion-Bombarded Nickel and Nickel Oxide. Spectr. Lett. 47(5) (2014) 363.
15. A. El Boujlaidi et al. Photon emission produced by Kr^+ ions bombardment of Cr and Cr_2O_3 targets. Nucl. Instrum. Methods B 343 (2015) 158.
16. A. Afkir et al. Angular distribution of particles sputtered from a copper target by 5-keV Kr ions: Experiment and simulation study. Surf. Interface Anal. 53(9) (2021) 792.
17. R. Jourdani et al. Effects of lithium insertion and deinsertion into V_2O_5 thin films: Optical, structural, and absorption properties. Surf. Interface Anal. 50(1) (2018) 52.
18. P.-G. Fournier et al. Angular distribution of sputtered particles and surface morphology: the case of

beryllium under a krypton beam at various incidences. Nucl. Instrum. Methods B 230 (2005) 577.
19. M. Ait El Fqih, P.-G. Fournier. Optical emission from Be, Cu and CuBe targets during ion beam sputtering. Nucl. Instrum. Methods B 267 (2009) 1206.
20. C.B. Kerkdijk, R. Kelly. Oxygen-dependent photon emission from Ne^+-bombarded Mg. Rad. Effects 38(1-2) (1978) 73.
21. P.G. Fournier et al. Light emission from Be and BeO surfaces bombarded by 5 keV Kr^+ ions. Nucl. Instrum. Methods B 249 (2006) 153.
22. A. Lawicki, A. Lawicka, K. Kreft. Luminescence in collisions of low-energy ions with graphite and Al_2O_3. Eur. Phys. J. Spec. Top. 144 (2007) 161.
23. A. El Boujlaidi et al. Continuum radiation emitted from transition metals under ion bombardment. Eur. Phys. J. D 66 (2012) 273.
24. A.A. Radzig, B.M. Smirnov. *Reference Data on Atoms, Molecules, and Ions* (Berlin, Heidelberg: Springer, 1985) 466 p.; *CRC Handbook of Chemistry and Physics.* D.R. Linde (ed.). 83rd ed. (Washington DC: CRC Press, 2002) 2664 p.
25. C.W. White, N.H. Tolk. Optical Radiation from Low-Energy Ion-Surface Collisions. Phys. Rev. Lett. 26 (1971) 486.
26. I. Terzić, B. Perović. Spectral analysis of light emitted from metallic targets bombarded by high energy ions. Surf. Sci. 21 (1970) 86.
27. A. Imanishi, E. Tsuji, Y. Nakato. Dependence of the Work Function of TiO_2 (Rutile) on Crystal Faces, Studied by a Scanning Auger Microprobe. J. Phys. Chem. C 111(5) (2007) 2128.
28. H. Wu, L.-S. Wang. Electronic structure of titanium oxide clusters: TiO_y(y = 1-3) and $(TiO_2)_n$ (n = 1-4). J. Chem. Phys. 107(20) (1997) 8221.
29. C.W. White et al. Continuum optical radiation produced by low-energy heavy particle bombardment of metal targets. Nucl. Instrum. Methods 132 (1976) 419.
30. D.J. Mowbray et al. Stability and Electronic Properties of TiO_2 Nanostructures with and without B and N Doping. J. Phys. Chem. C 113(28) (2009) 12301.
31. A. Afanasieva et al. Comparison of the main parameters of the ion-photon emission of titanium atoms and singly charged ions. Journal of Surface Investigation: X-ray, Synchrotron and Neutron Techniques 11(1) (2017) 146.
32. G. Blaise, G. Slodzian. Processus de formation d'ions à partir d'atomes éjectés dans des états électroniques surexcités lors du bombardement ionique des métaux de transition. J. Phys. France 31(1) (1970) 93.
33. C. Coudray, G. Slodzian. Contribution of the Landau-Zener-Stueckelberg model to the understanding of positive secondary-ion emission. Phys. Rev. B 49(14) (1994) 9344.
34. E.O. Rausch, A.I. Bazhin, E.W. Thomas. On the origin of broad band optical emission from Mo, Nb, and W bombarded by heavy ions. J. Chem. Phys. 65(11) (1976) 4447.
35. T. Kiyan, V.V. Gritsyna, Y. Fogel. On the continuous spectrum emitted by particles ejected from the surface of solid targets by an ion beam. Nucl. Instrum. Methods 132 (1976) 415.
36. A. Qayyum, M.N. Akhtar. Continuum light emission from sputtered species of graphite during ion beam irradiation. Eur. Phys. J. D 12 (2000) 181.

Л. Жадуаль[1], А. Афкір[1], А. Ель Бужлайді[1], М. Айт Ель Фкіх[2,*], Р. Журдані[1], А. Каддурі[1]

[1] Лабораторія матеріалів, енергії та навколишнього середовища, Університет Каді Айяд, Марракеш, Марокко
[2] Лабораторія штучного інтелекту та інженерії складних систем, Університет Хасана II Касабланки, Касабланка, Марокко

*Відповідальний автор: m.aitelfqih@gmail.com

ІОННО-ФОТОННЕ ВИПРОМІНЮВАННЯ ВІД ТИТАНОВОЇ МІШЕНІ ПІД ПУЧКОМ ІОНІВ

Експериментально досліджено випромінювання фотонів у діапазоні довжин хвиль 280 - 420 нм у результаті розпилення іонного пучка 5 Kr^+ з титану в присутності та відсутності кисню. Спостережені спектри складаються із серії дискретних ліній, накладених на широкосмуговий континуум. Дискретні лінії відносяться до збудженого нейтрального Ti I і збуджених іонів Ti II. Відмінності спостережених інтенсивностей спектральних ліній розглядаються з точки зору процесів перенесення електронів між збудженим розпиленим атомом і електронними рівнями твердого тіла. Процес радіаційної дисоціації та розрив хімічних зв'язків, по всій імовірності, сприяють посиленню інтенсивності випромінюваних фотонів. Спостерігається неперервне випромінювання, що, дуже ймовірно, пов'язане з електронною структурою титану. Колективна деактивація електронів 3d-оболонки відіграє певну роль в емісії цього випромінювання.

Ключові слова: розпилення, титан, світловипромінювання, модель переносу електронів, неперервне випромінювання.

Надійшла/Received 14.06.2021